2023

Final Lab Project

ME396, PROF. KOMPERDA

ALEKSANDAR DYULGEROV

I. Introduction

The strength of an engine is often linked to its exhaust system. In the study, a new design for an exhaust made of 316 Stainless Steel is evaluated. The primary focus is understanding its ability to manage heat and the flow of exhaust gases effectively. Using software tools like Fluent and ANSYS, gas flow patterns and temperature variations are examined. The objective is to determine the efficiency of the design and identify potential areas of improvement. The goal is achieving a design that excels in performance.

II. Problem Statement

The performance and integrity of a new exhaust manifold design constructed from 316 Stainless Steel under various operational conditions are simulated. Boundary conditions include an engine exhaust gas temperature of 525K, an under-hood temperature of 398K, and connections to the catalytic converter. Initial conditions involve an exhaust gas flow rate of 0.12kg/s for each of the three ports and a backpressure at the manifold outlet of 27kPa. Mesh statistics include 10601 nodes and 5199 elements for static structural and steady state thermal. Fluent mesh includes 19599 nodes and 48031 elements.

Metrics of interest include flow dynamics, temperature distribution, and physical stresses. Fig. 1 below shows how the solver modules are connected in FSI.

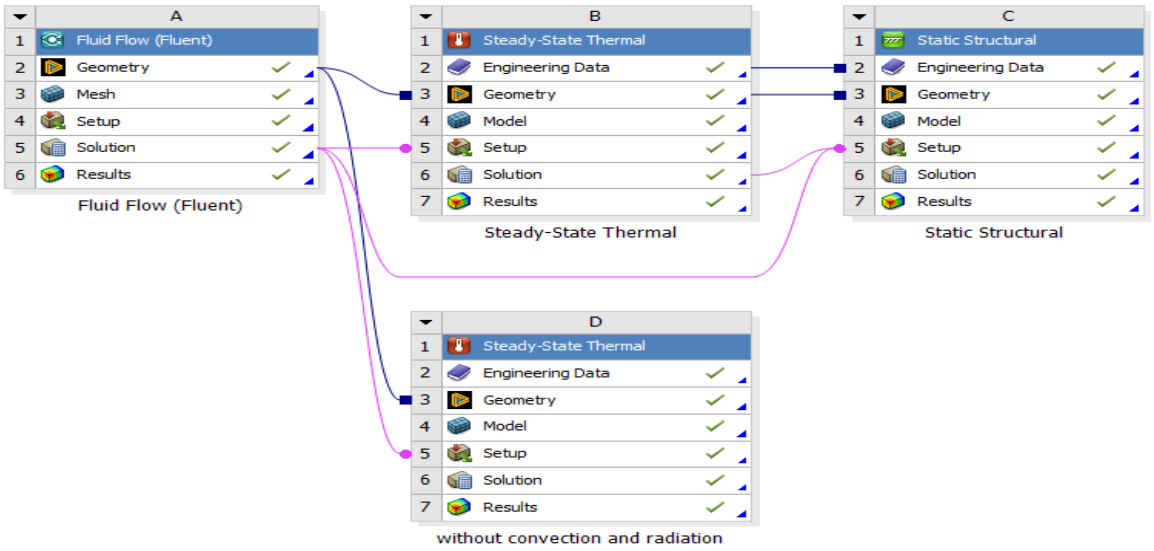

Figure 1: Solver Module Connections in FSI

III. Method

In Workbench, the Fluent cell was set up first since its solutions were linked to the steady-state thermal and static structural cells. Mesh generation was ensured to be under 50,000 elements/nodes with element sizing at 0.5m. The Fluent setup incorporated energy modeling, realizable and enhanced wall treatment, a 0.12 kg/s mass flow rate at each inlet port with normal to boundary flow, and exhaust gas was modeled as CO2.

The static structural setup involved adding fixed support for each of the screw holes at the inlet and outlets. The imported load of pressure and body temperature was used, and metrics for total deformation, equivalent stress, and safety factor were added. An imported pressure load applied to the inside faces came from the Fluent cell, and the thermal load for the entire body was also brought in.

For steady-state thermal, convection, radiation, and conduction were considered. Convection encompassed all faces, excluding the ones touching the engine and the catalytic converter. Radiation used the same face selection as convection. For conduction, the engine and catalytic converter faces were maintained at the designated temperature.

Lastly, the 316 Stainless Steel material initially lacked yield and compressive strength data, which was supplemented through the engineering data in the system panel.

IV. Results

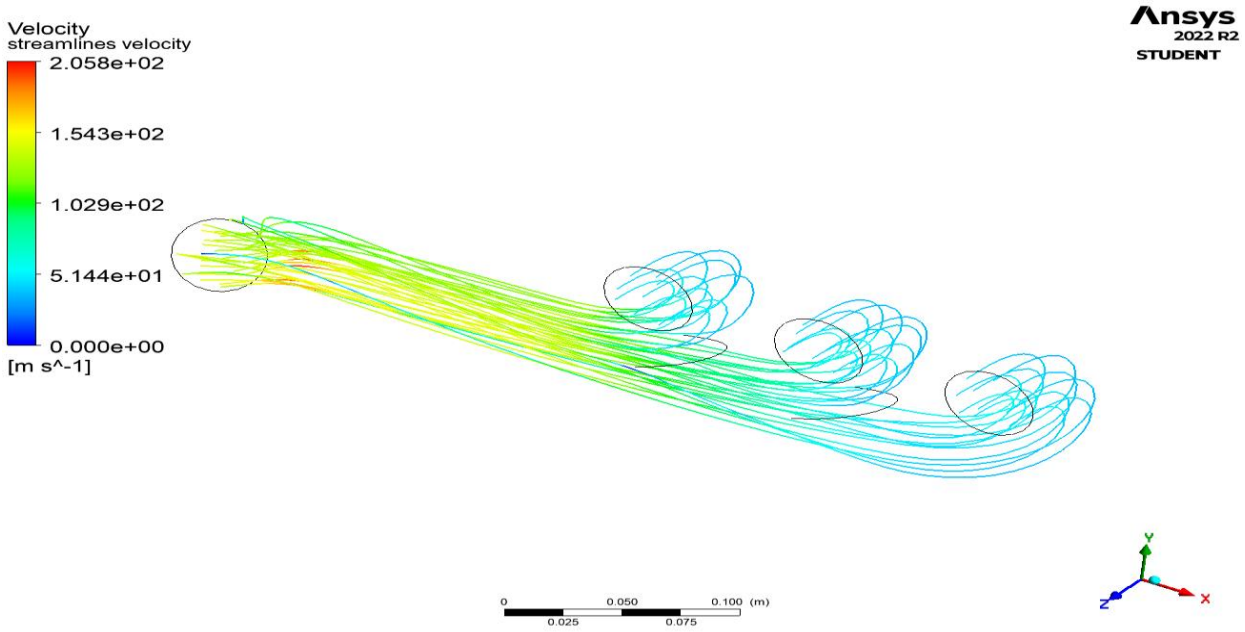

Figure 2: Velocity Streamline.

Fig. 2 shows the velocity streamline from the fluent cell of the three inlets with units of velocity being m/s.

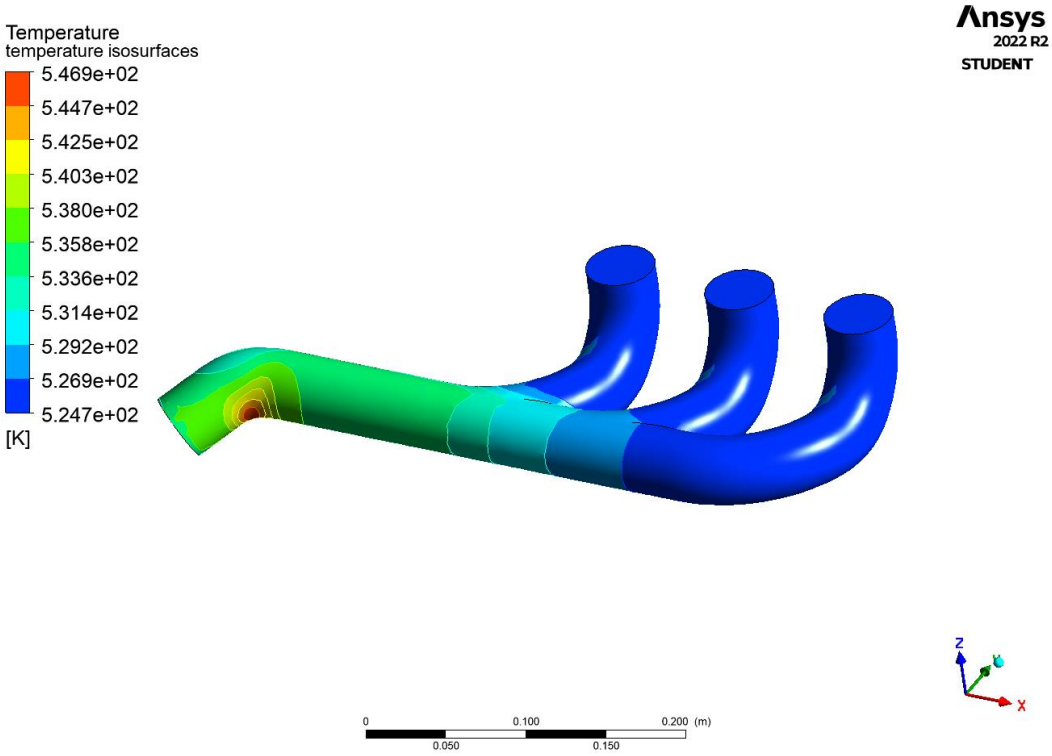

Figure 3: Temperature Isosurfaces.

Fig.3 shows the temperature gradient within the pipe structure is depicted by a transition from warmer hues (indicating higher temperatures) in the main segment to cooler hues (signifying lower temperatures) in the upward-bending branches. A pronounced hotspot in the main segment suggests areas of concentrated heat, possibly due to factors like increased friction or external heat sources. The cooler hues in the branches might result from reduced flow velocity or natural convection processes.

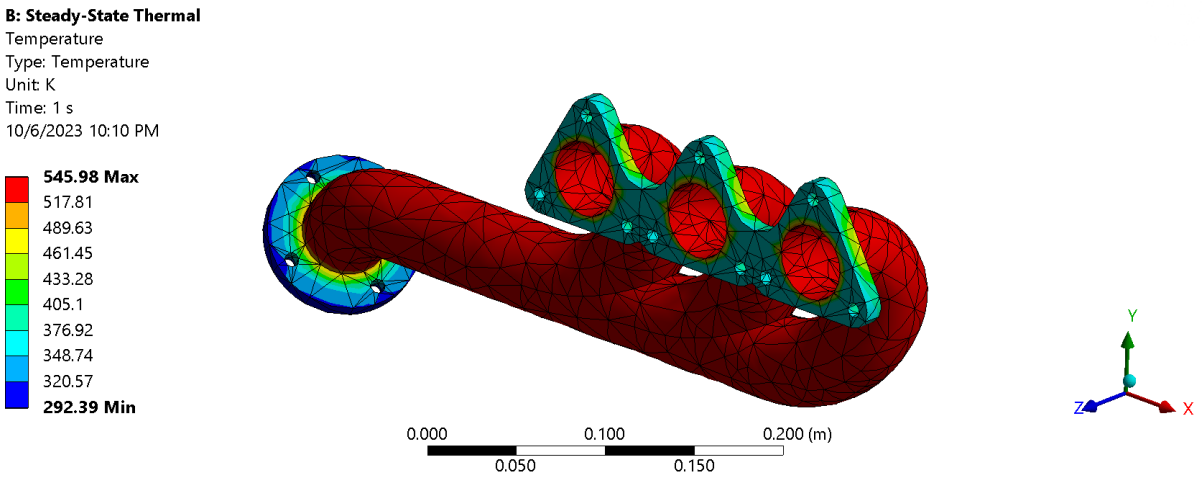

Figure 4: Temperature Distribution from Steady State Heat Transfer with convection and radiation.

In Fig. 4, the temperature distribution, measured in Kelvin, spans from a maximum of 545.98 K (indicated by red hues) to a minimum of 292.39 K (depicted by blue hues). The central elongated portion exhibits consistently high temperatures, while cooler regions are noticeable in the surrounding catalytic converter and inlet flanges.

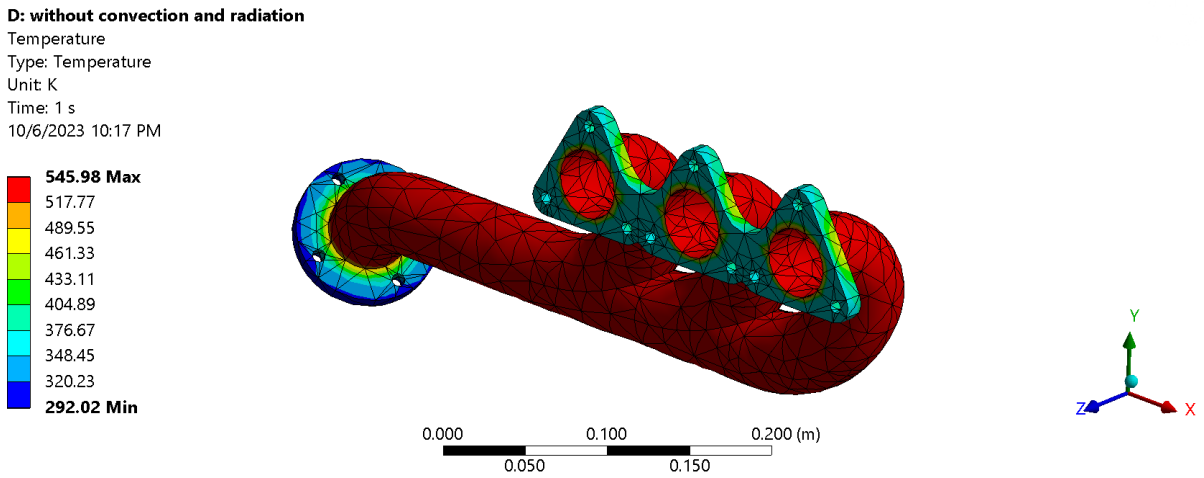

Figure 5 : Temperature Distribution from Steady State Heat Transfer without convection and radiation.

When convection and radiation boundary conditions were removed from the thermal cell simulation, the temperature distribution in Fig. 5 followed the same pattern as Fig. 4 and the min and max were not affected. This indicates that thermal losses due to convection/radiation are not significant. Therefore, radiation and convection can be neglected in the simulation.

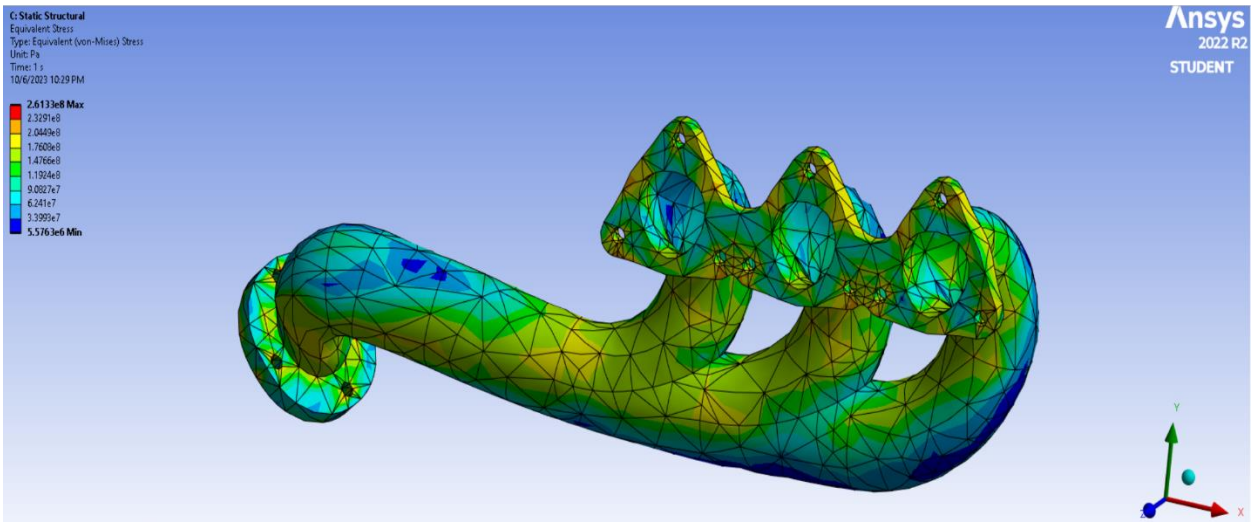

Figure 6: Von Mises Equivalent Stress from Static Structural

Fig. 6 shows stresses, measured in Pascals, range from a maximum of 2.613e8 Pa (represented by the red hues) to a minimum of 5.576e6 Pa (shown in blue). The elongated middle section exhibits moderate stress levels, while the surrounding spherical structures display both high and low stress regions. This stress distribution aids in pinpointing potential areas of concern and assessing the component's structural resilience.

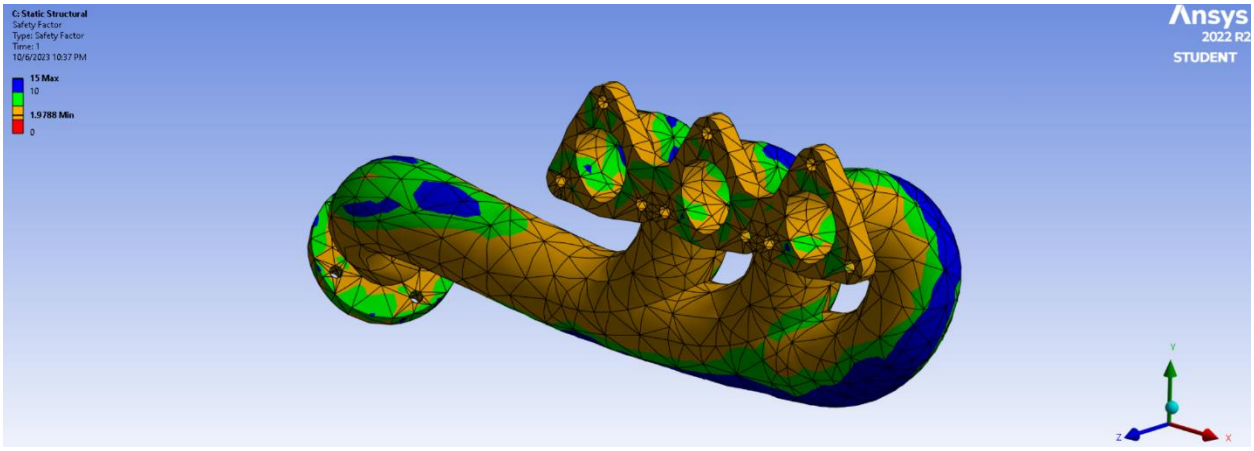

Figure 7: Safety Factor from Static Structural.

The safety factor of the exhaust manifold in Fig. 7 is 1.9788. This factor safety is nearly 2, an acceptable value for exhaust manifolds. With respect to the stress the manifold experiences and its failure and yield stress, the design does not need to be changed. The customer's design is sufficient.

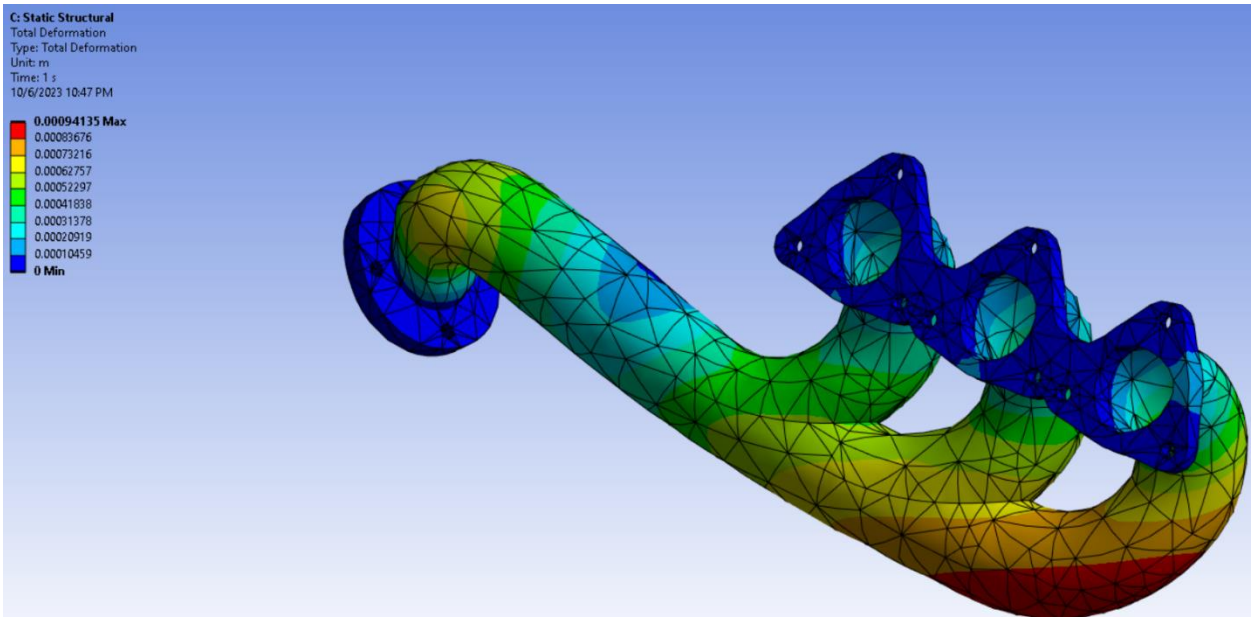

Figure 8: Total Deformation from Static Structural.

In Fig. 8, deformation values, quantified in meters, range from a maximum of 0.00094135 m (represented by the red hues) to a minimum of 0 m (shown in blue). Most noticeably the elongated section to the right in the figure shows the highest region of total deformation. The inlets and outlets are showing minimum total deformation.

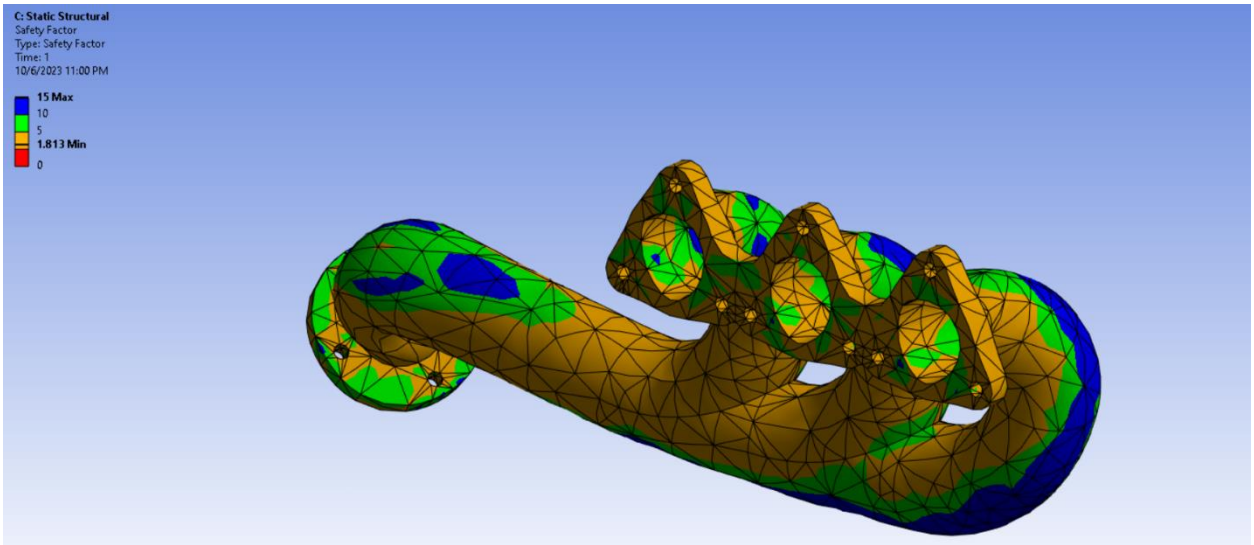

Figure 9: Safety Factor from Static Structural with convection and radiation ambient set to 50 K.

Changing the convection and radiation ambient temperature under-hood conditions to 50 K did not affect the safety factor. Altering these conditions does not improve the design's performance.

The catalytic converter end of the exhaust manifold was modeled using a temperature boundary condition at 295K. This seems a bit too low to be considered realistic. Instead, the average temperature after running the engine for a while should be taken into consideration. While the simulation's solutions and failures are accurate, they could be made better by using a higher temperature for the catalytic converter. More ranges in the 500K to 800K could be modeled to get a realistic interpretation of the simulation in real world conditions. For the structural boundary condition on the outlet side, the inner faces of where the bolts go were selected, then the faces were applied using a fixed support. Yes, this is a valid assumption. Exhaust manifolds are typically connected at this end using flanged connections, bolts, ball and socket, clamped or compression connections, and flex pipes.

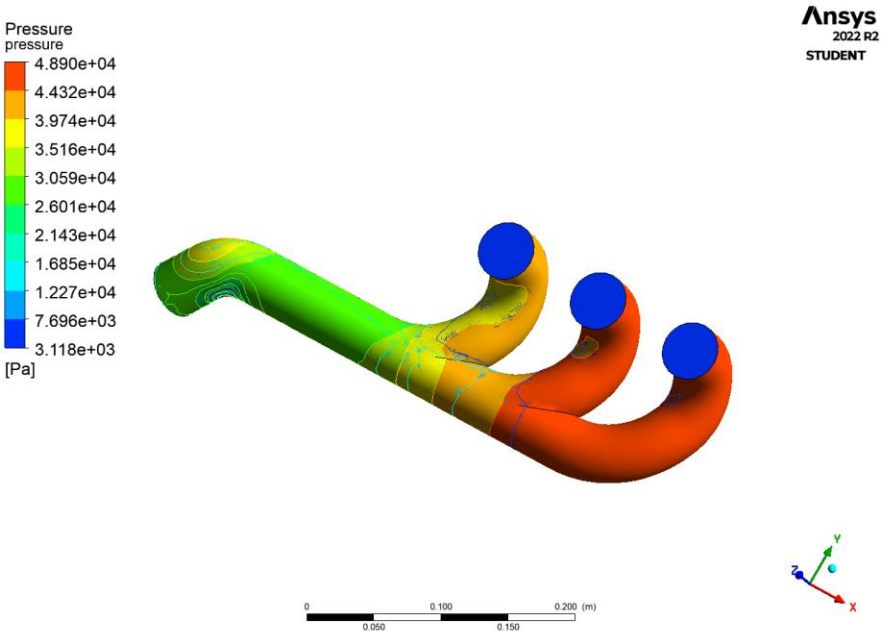

Figure 10: Pressure contour of the walls on the exhaust manifold.

Referencing Fig. 10, its abundantly clear the right-hand side of the exhaust manifold is experiencing 4.89e4 Pa regions of high pressure. Additionally, Fig. 8 showed high total deformation in that right side region. Even though the exhaust manifold meets a successful safety factor 2, anticipated failure would most likely occur due to high pressure concentrations in the right-side region of the exhaust manifold. Additionally, performance issues occur at the left-hand side of the outlet because there is a major spike in pressure. This is possibly due to turbulence effects and the sharp turn. To mitigate this, it's possible to make the edge smoother and a more gradual transition.

From Bernoulli's Equation

$$P_1 + \frac{1}{2}\rho v_1^2 + \rho g h_1 = P_2 + \frac{1}{2}\rho v_2^2 + \rho g h_2$$

Referencing Fig. 2, the velocity at the inlets could be further improved as they are showing lower velocities. One way of improving them is to decrease surface area in pipes. If the cross-sectional area of a pipe decreases (like in a nozzle), then the fluid velocity must increase to maintain constant mass flow rate according to the conservation of mass. Regarding Bernoulli's equation, when the fluid enters the inlet pipes, v2 will be greater than v1. The kinetic energy term (1/2pv^2) on the right-hand side will be greater than on the left side. To balance the equation, P_2 must be less than P_1. Thus, velocity increases in the constriction and pressure decreases.

V. Conclusion

The analysis of the 316 Stainless Steel exhaust manifold offered pivotal insights into its performance and structural attributes. The temperature distribution revealed that convection and radiation effects are minimal, simplifying future design considerations. Despite the manifold boasting a satisfactory safety factor, areas of high pressure and deformation on its right-side flag potential weaknesses. Lastly, flow dynamics at the inlets can be optimized further, leveraging principles from Bernoulli's equation to enhance performance.